


Ultranarrow Superradiant Lasing by Dark Atom-Photon Dressed States

 Yuan Zhang^{1,*,} Chongxin Shan,¹ and Klaus Mølmer^{2,†}

¹*Henan Key Laboratory of Diamond Optoelectronic Materials and Devices, Key Laboratory of Material Physics, Ministry of Education, School of Physics and Microelectronics, Zhengzhou University, Daxue Road 75, 450052 Zhengzhou, China*

²*Center for Complex Quantum Systems, Department of Physics and Astronomy, Aarhus University, Ny Munkegade 120, DK-8000 Aarhus C, Denmark*

 (Received 19 March 2020; revised 22 December 2020; accepted 22 February 2021; published 22 March 2021)

We show that incoherent pumping of an optical lattice clock system with ultracold strontium-88 atoms produces laser light with a ≈ 10 Hz linewidth when the atoms are exposed to a magnetic field. This linewidth is orders of magnitude smaller than both the cavity linewidth and the incoherent atomic decay and excitation rates. The narrow lasing is due to an interplay of multiatom superradiant effects and the coupling of bright and dark atom-light dressed states by the magnetic field.

DOI: 10.1103/PhysRevLett.126.123602

Introduction.—Conventional lasers rely on optical coherence established by stimulated emission from a population-inverted medium and they have a spectral linewidth set by the Schawlow-Townes limit [1]. In contrast, superradiant lasers rely on coherence in the atomic gain medium, established by the collective atom-light interaction, and they have a minimal linewidth given by the Purcell enhanced atomic decay rate Γ_c [2–6]. Recent experiments with ⁸⁸Sr alkaline earth atoms trapped in an optical lattice inside an optical cavity, see Fig. 1(a), show that the two lasing mechanisms may coexist in a superradiant crossover regime [7]. Theoretical studies [8,9] suggest that lasing in this regime benefits from both the optical and atomic coherence, and can achieve linewidths even smaller than Γ_c . To reach this regime, however, the atoms have to be pumped very hard, which is challenging in current experiments.

The same system was employed recently in [10] to demonstrate magnetic field-controlled transmission of a weak light probe. This phenomenon can be explained with a simple model of three-coupled oscillators [10,11], but it can also be ascribed to bright and dark atom-photon dressed states formed by coupling three-level atoms collectively with the optical cavity mode (see Supplemental Material [12], Secs. S1 and S2). In this Letter, we introduce incoherent pumping of the atoms, cf. the black solid and dashed arrows in Fig. 1(b), and we show that an ensemble of atoms with Zeeman-split excited states exhibits lasing with very narrow linewidth. This lasing relies on dark dressed states, and their influence on the lasing mechanism is not captured in previous studies dealing with two-level atoms [8,9], and it also differs fundamentally from the narrower transmission relying on dark states dressed by Raman beams [19]. Importantly, we show that the lasing is orders of magnitude narrower than the one relying on two-level atoms, and it can be achieved with pumping rates

compatible with current experiments. We expect that this new lasing mechanism will find applications with both strontium atoms [20,21] and other atoms like calcium [22] and ytterbium [23].

The physical system.—Figure 1(b) shows the singlet ground state 1S_0 , the triplet excited state 3P_1 , and a further excited state employed for incoherent excitation of the atoms. The spin-forbidden $^1S_0 - ^3P_1$ transition is weakly allowed in ⁸⁸Sr atoms due to state mixing by the spin-orbit

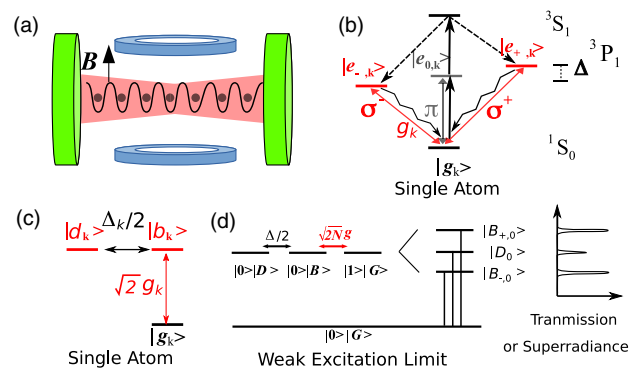


FIG. 1. Panel (a) illustrates thousands of ⁸⁸Sr atoms trapped in an optical lattice inside an optical cavity. Panel (b) shows the ground state (1S_0) and the three excited states (3P_1) of the k th atom, which are split due to a magnetic field. The atom is pumped (black solid arrows) to the highly excited state 3S_1 via the $e_{0,k}$ excited state and decays rapidly (dashed arrows) to the 3P_1 excited states $e_{\pm,k}$, and returns to the ground state by spontaneous emission (wavy arrows) or by the coherent coupling to the cavity mode (red thin double-head arrows). Panel (c) shows the coherent coupling to the cavity in the basis of bright and dark atomic excited states. Panel (d) shows the symmetric states of N atoms and the cavity field sharing a single excitation, and the corresponding atom-photon dressed eigenstates, which explain the three peaks in the transmission spectrum and in the steady-state lasing spectrum.

interaction [24]. In the presence of a static magnetic field, the 3P_1 level of the k th atom is split and the atom emits σ_{\pm} , π polarized light at different frequencies from the three Zeeman eigenstates $|e_{\pm,k}\rangle$, $|e_{0,k}\rangle$. Note that both the transitions σ_{\pm} couple to the single fundamental cavity mode with linear polarization in the horizontal direction.

The frequency of the $^1S_0 - ^3P_1$ transition is $\omega_a = 2\pi c/\lambda$ with the wavelength $\lambda = 689$ nm, and the excited state splitting is $\Delta_k = 2\pi \times 2.1B$ MHz, where the static magnetic field B is in units of gauss [10]. This yields the single atom Hamiltonian $H_{a,k} = \sum_{s=e_+,e_-} \hbar\omega_{s,k}|s_k\rangle\langle s_k|$, where $\omega_{e_{\pm,k}} = \omega_a \pm \Delta_k/2$. The coupling to the cavity mode is given in the rotating wave approximation by $H_{a-c,k} = \hbar g_k(|e_{+,k}\rangle\langle g_k| + |e_{-,k}\rangle\langle g_k|)a + \text{H.c.}$ Here and in the following, we assume identical atoms, i.e., $\Delta = \Delta_k$ and $g = g_k = 2\pi \times 7.5$ kHz for all atoms. The cavity mode is described by the Hamiltonian $H_c = \hbar\omega_c a^\dagger a$ with the frequency ω_c , and creation a^\dagger and annihilation operators a . We ignore contributions from the excited state $|e_{0,k}\rangle$ since it does not couple to the cavity mode.

We shall refer to $|d_k\rangle = (|e_{+,k}\rangle - |e_{-,k}\rangle)/\sqrt{2}$ and $|b_k\rangle = (|e_{+,k}\rangle + |e_{-,k}\rangle)/\sqrt{2}$ as the dark and bright excited states (note that $|d_k\rangle$ does not couple to the cavity mode). The single atom-cavity interaction Hamiltonian can then be written as $H_{a-c,k} = \hbar\sqrt{2}g_k|b_k\rangle\langle g_k|a + \text{H.c.}$, and the atomic Hamiltonian $H_{a,k} = \hbar\omega_a(|b_k\rangle\langle b_k| + |d_k\rangle\langle d_k|) + \hbar(\Delta/2)(|b_k\rangle\langle d_k| + |d_k\rangle\langle b_k|)$ couples the dark and bright states via the magnetic field-induced Zeeman splitting Δ_k , see Fig. 1(c). The total system is subject to the Hamiltonian $H_s = H_c + \sum_k(H_{a,k} + H_{a-c,k})$, and explores a Hilbert space composed of photon number states $|n\rangle$ and collectively excited atomic states. In the low excitation limit, the atomic ground state $|G\rangle = \prod_k |g_k\rangle$ and the collective singly excited bright state $|B\rangle = N^{-1/2} \sum_k |b_k\rangle \prod_{j \neq k} |g_j\rangle$ and dark state $|D\rangle = N^{-1/2} \sum_k |d_k\rangle \prod_{j \neq k} |g_j\rangle$ yield a series of atom-photon dressed states, see Sec. S1 in [12]. The lowest dressed states shown in Fig. 1(d) explain the triplet features in the transmission experiments [10], see Sec. S2 in [12]. In this Letter, we show that the atom-light dressed states also lead to steady-state lasing, featuring a similar triplet spectrum with an ultranarrow central peak.

Master equation.—To study the steady-state emission from the system with incoherently pumped atoms, we employ the Lindblad master equation, which also accounts for photon loss and atomic spontaneous emission (see Sec. S3 of [12]):

$$\begin{aligned} \frac{\partial}{\partial t}\rho = & -\frac{i}{\hbar} \left[H_c + \sum_k (H_{a,k} + H_{a-c,k}), \rho \right] - \kappa \mathcal{D}[a]\rho \\ & - \sum_k \gamma_k (\mathcal{D}[A_{gb}^k]\rho + \mathcal{D}[A_{gd}^k]\rho) \\ & - \sum_k \eta_k (\mathcal{D}[A_{bg}^k]\rho + \mathcal{D}[A_{dg}^k]\rho). \end{aligned} \quad (1)$$

Here, for notational purposes, we have introduced the atomic operators $A_{st}^k = |s_k\rangle\langle t_k|$ ($s, t = g, b, d$). The dissipation superoperator $\mathcal{D}[o]\rho = \{o^\dagger o \rho + o \rho o^\dagger - o \rho - \rho o\}/2$ with different operators o , describes the cavity loss with the rate $\kappa = 2\pi \times 150$ kHz, the atomic spontaneous emission with rate $\gamma = \gamma_k = 2\pi \times 7.5$ kHz, and the incoherent atomic excitation with rate $\eta = \eta_k$, obtained, e.g., via excitation of higher short-lived excited states, see Fig. 1(b) and Sec. S4 in [12]. We ignore the negligible pure dephasing of the atoms in the optical lattice clock system.

To solve the master equation for thousands of atoms, we utilize a cluster expansion approach [25] equivalent to a second-order mean-field theory [2,9]. In this approach, we employ the equation $\partial\langle o \rangle/\partial t = \text{tr}\{o\partial\rho/\partial t\}$ for the expectation value $\langle o \rangle = \text{tr}\{o\rho\}$ of any observable o of interest, and use Eq. (1), to express the right hand side in terms of mean values of other observables, see Sec. S3 of [12]. It turns out that the mean photon number in the cavity $\langle a^\dagger a \rangle$ couples to the atom-photon correlations $\langle a A_{st}^k \rangle$, which in turn couple to the atom-atom correlations $\langle A_{st}^k A_{s't'}^{k'} \rangle$ ($k \neq k'$) and third-order correlations such as $\langle a^\dagger a A_{st}^k \rangle$. To truncate the hierarchy of equations, we approximate third-order quantities with products of lower-order terms, e.g., $\langle a^\dagger a A_{st}^k \rangle = \langle a^\dagger a \rangle \langle A_{st}^k \rangle + \langle a^\dagger \rangle \langle a A_{st}^k \rangle + \langle a^\dagger A_{st}^k \rangle \langle a \rangle - 2\langle a^\dagger \rangle \langle a \rangle \langle A_{st}^k \rangle$, resulting in closed nonlinear equations. Assuming identical properties for all atoms, we note that $\langle A_{st}^k \rangle$ and $\langle a A_{st}^k \rangle$ are the same for all k , and $\langle A_{st}^k A_{s't'}^{k'} \rangle$ are identical for all pairs (k, k') . This allows us to reduce the number of independent elements to 102. Since we do not inject a mean field into the system, the mean values of the cavity field annihilation operator $\langle a \rangle$ and the atomic transition operators $\langle A_{st}^k \rangle$ ($s \neq t$ with $s = g$ or $t = g$) vanish for all times and thus the set of equations is further reduced. All relevant mean values can thus be readily found numerically. By applying second-order mean field theory, we incorporate manifestly nonvanishing correlations while we do not rely on the spontaneous symmetry breaking ansatz in first-order mean field theory. Higher-order corrections to the theory are expected to be negligible [26] in the limit of many atoms, and the approach has, indeed, been applied to study steady-state superradiance [3] and Dicke superradiance phase transition [27] with two-level atoms, where it has also been validated by comparison with exact results for finite systems.

Magnetic field-controlled superradiant lasing.—We solve the equations for atoms that are continuously pumped to the excited states with the rate η , e.g., by excitation of the short-lived higher excited state in Fig. 1(b). Figures 2(a) and 2(b) show the dependence of the system steady state on η for a finite Zeeman coupling $\Delta/2\pi = 0.3$ MHz. Figure 2(a) shows that the steady-state population of the atomic ground state (black solid line) and the dark excited state (blue dotted line) decrease and increase with increasing η , while the bright excited state population (red dashed line) first increases and then decreases when $\eta > \gamma$.

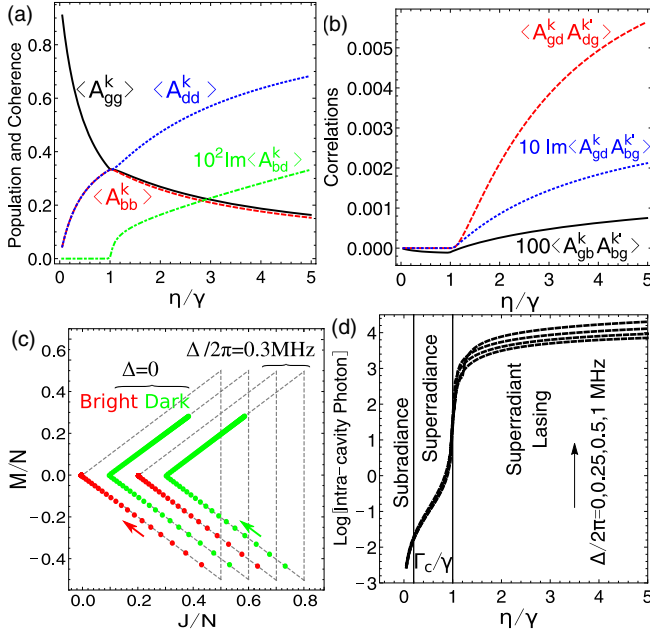


FIG. 2. Dependence of the steady state of 2.5×10^5 atoms on the atomic excitation rate η (relative to the decay rate γ). Panel (a) shows the population $\langle A_{gg}^k \rangle$ (black solid line), $\langle A_{bb}^k \rangle$ (red dashed line), $\langle A_{dd}^k \rangle$ (blue dotted line) of the ground state, the bright excited state and the dark excited state, respectively, as well as the imaginary part of the bright-dark state's coherence $\langle A_{bd}^k \rangle$ (green dot-dashed line). Panel (b) shows the correlations $\langle A_{gb}^k A_{bg}^k \rangle$ (black solid line), $\langle A_{gd}^k A_{dg}^k \rangle$ (red dashed line), and $\text{Im}\langle A_{gd}^k A_{bg}^k \rangle$ (blue dotted line) of the atoms ($k \neq k'$) related to the dark and bright transitions. In panels (a) and (b) the Zeeman splitting is $\Delta/2\pi = 0.3$ MHz. Panel (c) shows a representation of the multiply excited atomic states by pseudo-Dicke collective quantum numbers J_s, M_s of the bright $s = b$ (red dots) and dark $s = d$ (green dots) transition for increasing η (arrows) for the system with $\Delta = 0$ (left) and $\Delta = 2\pi \times 0.3$ MHz (right). The results are shifted for clarity and the dashed lines indicate the boundaries of each triangle of Dicke ladders. Panel (d) shows the intracavity photon number as a function of η for different values of the Zeeman coupling Δ . Other parameters are specified in the text.

The coherence between the bright and dark excited state (green dot-dashed line) first vanishes and then shows a thresholdlike behavior at $\eta = \gamma$. Figure 2(b) shows that the correlations between different atoms also start increasing for $\eta > \gamma$ for the bright transitions (black solid line), the dark transitions (red dashed line), and different transitions (blue dotted line). The former correlations reflect the collective coupling of the bright atomic transitions with the cavity mode, while the latter ones reflect the cavity-mediated interaction between the bright and dark transitions. In the absence of the Zeeman coupling, the correlations involving the dark states vanish (not shown).

The collective excitations of an ensemble of two-level systems can be described by Dicke states $|J, M\rangle$ [28],

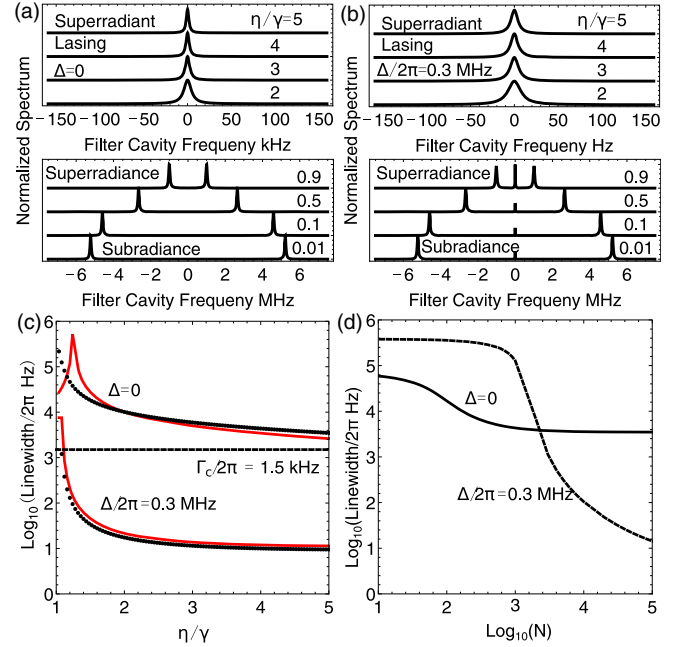


FIG. 3. Magnetic field-controlled subradiance, superradiance, and superradiant lasing. Panels (a) and (b) show the normalized steady-state spectra for increasing pumping η (relative to the decay rate γ), without ($\Delta = 0$) and with Zeeman coupling $\Delta/2\pi = 0.3$ MHz for systems with $N = 2.5 \times 10^5$ atoms [note that in the upper panel of (b) the frequency scale is in Hz]. (c) and (d) show the emission linewidth of the systems without and with Zeeman coupling as function of η/γ ($N = 2.5 \times 10^5$), and number of atoms N ($\eta/\gamma = 5$), respectively. In panel (c), the black dots and the red curves are the accurate results and those calculated with Eq. (2), respectively, and the black horizontal dotted line indicates the Purcell rate Γ_c . Other parameters are specified in the text.

where J and $M = -J, \dots, J$ represent the eigenvalues of collective spin operators associated with the two-level systems. The energy levels of the Dicke states for a given J form a vertical ladder with equal spacing (equal to the transition energy), and the states with different J can be shown as shifted vertical ladders forming a triangle pattern. Here, we adapt this concept to three-level systems by treating the bright $b_k \rightarrow g_k$ and dark $d_k \rightarrow g_k$ transitions as separate two-level transitions and then calculating the mean values J_s, M_s ($s = b, d$) for the pseudo Dicke states $|J_s, M_s\rangle$, see Sec. S5 of [12] for more details.

Figure 2(c) compares the evolution of the ensemble excitation with increasing pumping η for the system without (left) and with (right) the Zeeman coupling (magnetic field). We see that as η increases, the bright transition explores (red dots) the lower rung of subradiant Dicke states but terminates at the states with $J_b, M_b \approx 0$ due to the balanced stimulated absorption and emission, while the dark transition does not undergo these processes and thus explores (green dots) also states with $J_d \geq M_d > 0$ for $\eta > \gamma$. As these excited states do not couple to the cavity,

they are spectators to the system dynamics. When we include the magnetic field, however, they will couple to the cavity field via the bright states and give rise to narrow-linewidth lasing (see below).

The excited atomic ensemble releases its energy by emitting photons into the cavity, see Fig. 2(d). There are abundant studies on the superradiance and superradiant lasing by atoms with only a single excited state [2–5], but less effort is devoted to the radiation from the atoms with two or more excited states. Figure 2(d) verifies that in the absence of Zeeman coupling $\Delta = 0$, the three-level atoms behave like two-level systems as expected since the dark atomic excited state couples with neither the bright atomic excited state nor the cavity mode. As discussed in Refs. [9,29], this system undergoes transitions from subradiance to superradiance and finally to superradiant lasing as the pumping strength η overcomes the Purcell enhanced decay rate $\Gamma_c = 4g^2/\kappa = 2\pi \times 1.5$ kHz and the atomic decay rate γ , respectively, see the lower curve in Fig. 2(d) for $\Delta = 0$. In contrast, by introducing a finite Zeeman coupling Δ , the intracavity photon number changes significantly. In particular, for strong pumping $\eta > \gamma$, a finite value of Δ makes the photon number increase by about a factor of 10. More importantly, the Zeeman coupling has dramatic influence on the lasing spectrum.

The spectrum of radiation can be determined by applying the quantum regression theorem to the system master equation, but it can also be computed by coupling the cavity output to a narrow-linewidth filter cavity. In the latter case, the spectrum corresponds to the photon number in that cavity as a function of its frequency, which can be calculated easily with the cluster expansion method [9], see Secs. S6 and S7 of [12]. Figure 3(a) shows the emission spectrum for a system with 2.5×10^5 atoms in the absence of Zeeman coupling $\Delta = 0$. For weak pumping, the two peaks in the spectrum can be attributed to transitions between the lowest bright dressed states and the ground state in Fig. 1(d). For stronger pumping, the peaks approach each other and ultimately merge into a single peak. This behavior occurs because the atomic ensemble explores the collective Dicke-like states with a lower symmetry (lower J_s) for stronger pumping, and hence experiences a reduced effective collective coupling with the cavity mode, see Fig. 2(c) and Refs. [9,30,31].

Figure 3(b) shows that by introducing the finite Zeeman coupling $\Delta/2\pi = 0.3$ MHz, we modify the spectrum significantly. For weak pumping η , we find a new peak in the spectrum around the cavity mode frequency, which can be attributed to the transition between the dark dressed state and the ground state in Fig. 1(d). As η increases, the side peaks become weaker while the center peak gets stronger and more narrow. For more results on the influence of Δ , see Fig. S4(a) of [12]. We note that the Dicke state evolution of the dark and bright atomic transitions is very similar for systems with and without Zeeman coupling, see

Fig. 2(c), but the weak Zeeman coupling permits release of the energy of the dark excited states as light with an ultranarrow spectrum.

The effect of the Zeeman coupling is striking in Fig. 3(c), where we compare the spectrum linewidth for the system with Zeeman coupling $\Delta = 0$ (upper black dots) and $\Delta/2\pi = 0.3$ MHz (lower black dots). Here, we consider pumping rates $\eta > \gamma$ so that there is only a single dominant peak in the spectrum. Remarkably, with increasing η , the linewidth decreases to nearly $2\pi \times 10$ Hz for $\Delta \neq 0$, which is orders of magnitude smaller than $2\pi \times 4$ kHz obtained for $\Delta = 0$. This linewidth is also orders of magnitude smaller than the atomic decay rate of $2\pi \times 7.5$ kHz, the pumping rate of (up to) $2\pi \times 37.5$ kHz, the cavity loss rate of $2\pi \times 150$ kHz and the Purcell decay rate $\Gamma_c = 2\pi \times 1.5$ kHz.

To characterize the origin of the ultranarrow lasing, we have derived a semianalytical expression:

$$\Gamma = \frac{\kappa - \theta[(\gamma + 2\eta)(\langle A_{bb}^k \rangle - \langle A_{gg}^k \rangle) - \Delta \text{Im}\langle A_{db}^k \rangle]}{2 + \theta(\langle A_{bb}^k \rangle - \langle A_{gg}^k \rangle)}, \quad (2)$$

with the parameter $\theta = 8Ng^2/[(\gamma + 2\eta)^2 + \Delta^2]$, see Sec. S8 of [12]. Figure 3(c) shows that Eq. (2) (red curves) reproduces the accurate numerical results (black dots) very well. Equation (2) indicates that in the absence of Zeeman coupling $\Delta = 0$ the linewidth depends only on the population inversion $\langle A_{bb}^k \rangle - \langle A_{gg}^k \rangle > 0$ between the bright excited state and the ground state, while for $\Delta \neq 0$ it depends crucially on the coherence $\langle A_{db}^k \rangle$ between the bright and dark excited state. For the optimal pumping rate η and Zeeman coupling Δ , we observe an almost perfect cancellation of these contributions in the numerator of Eq. (2), leading to the ultranarrow spectrum, see Fig. S4(c) in [12].

For weak pumping, the spectrum is explained by the three atom-light dressed states formed by the singly excited states of the atom-cavity system, see Fig. 1(d), and it is consistent that for strong pumping, the ultranarrow spectrum is due to the atom-light dressed states formed by the highly excited states of the system. It is difficult to definitely discern the role of superradiant and collective effects, but we recall from our introduction that superradiant lasing exploits the coherence stored both in the gain medium and in the cavity field, and hence one would expect a reduction of the linewidth as function of increased atom number N , similar to the Schawlow-Townes linewidth scaling as $1/\bar{n}$ with the mean photon number \bar{n} in the conventional laser model. In Fig. 3(d) we show the spectrum linewidth as function of N for the pumping $\eta/\gamma = 5$ and the Zeeman splitting $\Delta/2\pi = 0, 0.3$ MHz. For $N > 10^3$ and $\Delta/2\pi = 0.3$ MHz, we indeed observe a drastic reduction of the linewidth, which approaches a few Hz and is orders of magnitude smaller than that for $\Delta = 0$.

In Sec. S9 of [12], we find that the lasing frequency partly follows variations in the cavity resonance frequency. To avoid broadening of the lasing spectrum due to this cavity-pulling effect, it is thus necessary to stabilize the cavity mode frequency to the same order of magnitude as the desired lasing signal.

Conclusion.—We have presented a novel scheme for superradiant lasing based on atom-photon dressed states, which are formed by dark atomic excited state and cavity photon states and populated by incoherent atomic excitation. The energy in these states is released to the cavity mode by a magnetic field-induced Zeeman coupling to the bright atomic excited states. The linewidth of the radiation is governed by the dark states and is therefore orders of magnitude more narrow than for the superradiant lasing based on (bright) two-level transitions.

We have employed a cluster expansion approach and analytical approximations to the problem, and we note a resemblance between our lasing mechanism and lasing without inversion [32]. This includes, see Sec. S10 of [12], the presence of strong coupling that leads to both well-separated dressed states and coherence in the system and to probe field amplification due to transitions among the dressed states. In our system, the dark and bright dressed states are formed due to the collective coupling to the quantized cavity field and the Zeeman coupling, and the incoherent atomic pumping drives the population and coherence dynamics and hence the emission by the system. We also see a possibly fruitful connection to the observation of undamped eigenmodes in coupled systems subject to gain and loss [33,34]. The analyses of these systems may inspire analytical approaches that incorporate both the dark state mechanism and multiatom collective effects and they may stimulate search for further applications of the mechanisms reported here.

This work was supported by the National Science Foundation of China through Project No. 12004344 and the Carlsberg Foundation through the Semper Ardens Research Project QCool and by the Danish National Research Foundation through the Center of Excellence for Complex Quantum Systems (Grant agreement No. DNRF156). The authors thank David Hunger and Stefan Schäffer for advice on the frequency stability of optical cavities, and Klemens Hammerer for discussion on the cluster-expansion approach.

*yzhuardipc@zzu.edu.cn

†moelmer@phys.au.dk

- [1] A. L. Schawlow and C. H. Townes, *Phys. Rev.* **112**, 1940 (1958).
 [2] D. Meiser, J. Ye, D. R. Carlson, and M. J. Holland, *Phys. Rev. Lett.* **102**, 163601 (2009).

- [3] D. Meiser and M. J. Holland, *Phys. Rev. A* **81**, 033847 (2010).
 [4] M. A. Norcia, M. N. Winchester, J. R. K. Cline, and J. K. Thompson, *Sci. Adv.* **2**, e1601231 (2016).
 [5] J. G. Bohnet, Z. Chen, J. M. Weiner, D. Meiser, M. J. Holland, and J. K. Thompson, *Nature (London)* **484**, 78 (2012).
 [6] H. Liu, S. B. Jäger, X. Yu, S. Touzard, A. Shankar, M. J. Holland, and T. L. Nicholson, *Phys. Rev. Lett.* **125**, 253602 (2020).
 [7] M. A. Norcia and J. K. Thompson, *Phys. Rev. X* **6**, 011025 (2016).
 [8] D. A. Tieri, M. Xu, D. Meiser, J. Cooper, and M. J. Holland, *arXiv:1702.04830*.
 [9] K. Debnath, Y. Zhang, and K. Mølmer, *Phys. Rev.* **98**, 063837 (2018).
 [10] M. N. Winchester, M. A. Norcia, J. R. K. Cline, and J. K. Thompson, *Phys. Rev. Lett.* **118**, 263601 (2017).
 [11] Z. X. Liu, B. Wang, C. Kong, H. Xiong, and Y. Wu, *Appl. Phys. Lett.* **112**, 111109 (2018).
 [12] See Supplemental Material at <http://link.aps.org/supplemental/10.1103/PhysRevLett.126.123602> for extra theoretical derivations, numerical simulations, and discussions, which includes Refs. [13–18].
 [13] E. T. Jaynes and F. W. Cummings, *Proc. IEEE* **51**, 89 (1963).
 [14] M. A. Norcia, J. R. K. Cline, J. A. Muniz, J. M. Robinson, R. B. Hutson, A. Goban, G. E. Marti, J. Ye, and J. K. Thompson, *Phys. Rev. X* **8**, 021036 (2018).
 [15] J. F. S. Brachmann, H. Kaupp, T. W. Hänsch, and D. Hunger, *Opt. Express* **24**, 21205 (2016).
 [16] M. Khudaverdyan, W. Alt, I. Dotsenko, T. Kampschulte, K. Lenhard, A. Rauschenbeutel, S. Reick, K. Schörner, A. Widera, and D. Meschede, *New J. Phys.* **10**, 073023 (2008).
 [17] Y. Zhu, *Phys. Rev. A* **45**, R6149 (1992).
 [18] G. Yang, Z. Tan, B. Zou, and Y. Zhu, *Opt. Lett.* **39**, 6695 (2014).
 [19] G. Dong, D. Xu, and P. Zhang, *Phys. Rev. A* **102**, 033717 (2020).
 [20] S. A. Schäffer, M. Tang, M. R. Henriksen, A. A. Jørgensen, B. T. R. Christensen, and J. W. Thomsen, *Phys. Rev. A* **101**, 013819 (2020).
 [21] C.-C. Chen, S. Bennetts, R. G. Escudero, B. Pasquiou, and F. Schreck, *Phys. Rev. Applied* **12**, 044014 (2019).
 [22] C. W. Oates, F. Bondu, R. W. Fox, and L. Hollberg, *Eur. Phys. J. D* **7**, 449 (1999).
 [23] N. Hinkley, A. Sherman, N. Phillips, M. Schioppo, N. D. Lemke, K. Beloy, M. Pizzocaro, C. W. Oates, and A. D. Ludlow, *Science* **341**, 1215 (2013).
 [24] M. M. Boyd, Ph.D. thesis, High precision spectroscopy of strontium in an optical lattice: Towards a new standard for frequency and time, University of Washington, 2007.
 [25] H. A. M. Leymann, A. Foerster, and J. Wiersig, *Phys. Rev. B* **89**, 085308 (2014).
 [26] A. Roth, Ph.D. thesis, Collective effects and superradiance in atomic ensembles, Leibniz University of Hannover, 2018.
 [27] P. Kirton and J. Keeling, *Phys. Rev. Lett.* **118**, 123602 (2017).
 [28] R. H. Dicke, *Phys. Rev.* **93**, 99 (1954).

- [29] M. Xu, D. A. Tieri, E. C. Fine, J. K. Thompson, and M. J. Holland, *Phys. Rev. Lett.* **113**, 154101 (2014).
- [30] Y. Zhang, Y. X. Zhang, and K. Mølmer, *New J. Phys.* **20**, 112001 (2018).
- [31] N. Shammah, S. Ahmed, N. Lambert, S. DeLiberato, and F. Nori, *Phys. Rev. A* **98**, 063815 (2018).
- [32] J. Mompart and R. Corbalán, *J. Opt. B* **2**, R7 (2000).
- [33] R. El-Ganainy, K. G. Makris, M. Khajavikhan, Z. H. Musslimani, S. Rotter, and D. N. Christodoulides, *Nat. Phys.* **14**, 11 (2018).
- [34] D. D. Smith, H. Chang, L. Horstman, and J.-C. Diels, *Opt. Express* **27**, 34169 (2019).